Journal of Macromolecular Science, Part A
Publication details, including instructions for authors and subscription information:
http://www.informaworld.com/smpp/title~content=t713597274

Solvent and Concentration-Dependent Aggregation Study of C60 Dyads and Multiads on Nonlinear Photonic Properties

K.H. Vincent Lau[a]; Robinson Anandakathir[b]; Kenneth Pritzker[a]; Long Y. Chiang[b]
[a] Department of Pathology and Laboratory Medicine, Mount Sinai Hospital and University of Toronto, Toronto, Canada [b] Department of Chemistry, University of Massachusetts Lowell, Lowell, MA

To cite this Article Vincent Lau, K.H. , Anandakathir, Robinson , Pritzker, Kenneth and Chiang, Long Y.(2008) 'Solvent and Concentration-Dependent Aggregation Study of C60 Dyads and Multiads on Nonlinear Photonic Properties', Journal of Macromolecular Science, Part A, 45: 11, 892 — 898
To link to this Article: DOI: 10.1080/10601320802378418
URL: http://dx.doi.org/10.1080/10601320802378418

Journal of Macromolecular Science®, Part A: Pure and Applied Chemistry (2008) **45**, 892–898

ISSN: 1060-1325 print / 1520-5738 online
DOI: 10.1080/10601320802378418

Taylor & Francis
Taylor & Francis Group

Solvent and Concentration-Dependent Aggregation Study of C_{60} Dyads and Multiads on Nonlinear Photonic Properties

K. H. VINCENT LAU[1], ROBINSON ANANDAKATHIR[2], KENNETH PRITZKER[1] and LONG Y. CHIANG[2]

[1]*Department of Pathology and Laboratory Medicine, Mount Sinai Hospital and University of Toronto, Toronto, Canada*

[2]*Department of Chemistry, University of Massachusetts Lowell, Lowell, MA 01854*

We have studied the molecular self-assembly tendency of C_{60}(>DPAF-C_9) dyad, C_{60}(>DPAF-C_9)$_2$ triad, and C_{60}(>DPAF-C_9)$_4$ pentads in a solvent-dependent and concentration-dependent manner. The evaluation was performed by the particle-size measurements on molecular assemblies in either toluene or CS_2 using the dynamic light scattering technique. As a result, we observed a strong bimodal particle size distribution in most cases of the samples in both nonpolar solvents. In the instance of C_{60}(>DPAF-C_9) dyad, the first group of small nanoparticles exhibited a particle diameter size of 3.0–4.0 nm in good agreement with the estimated long axis length of C_{60}(>DPAF-C_9) (~2.7 nm), using 3D molecular modeling technique. Similar observation of a bimodal particle size distribution was detected on C_{60}(>DPAF-C_9)$_4$ pentads in toluene with a small nanoparticle diameter size of ~8.0 nm fitting well with the estimated dimension length of ~9.8 nm for loosely packed 3–6 C_{60}(>DPAF-C_9)$_4$ molecular assemblies. Furthermore, the tendency of forming large aggregation particles in a particle diameter of more than 4.0 μm was significantly enhanced at a concentration of 1.0×10^{-2} M.

Keywords: [60]fullerenyl monoadduct, [60]fullerenyl bisadduct, [60]fullerenyl tetraadduct, concentration-dependent aggregation, zetasizer measurement.

1. Introduction

A series of C_{60}-*keto*-DPAF-C_9 assembly nanomaterials, where DPAF-C_9 represents 9,9-di(3,5,5-trimethylhexyl)-2-diphenylaminofluorene, including the monoadduct C_{60}(>DPAF-C_9), the bisadducts C_{60}(>DPAF-C_9)$_2$, and the tetraadducts C_{60}(>DPAF-C_9)$_4$ were synthesized and extensively studied recently for their nonlinear photonic properties (1–4). All of these nanomaterials were found to exhibit large two-photon absorption (2PA) cross-sections in femtosecond (fs) and picosecond (ps) regions (3). Especially, both C_{60}(>DPAF-C_9)$_2$ triads and C_{60}(>DPAF-C_9)$_4$ pentads gave nonlinear light transmittance reduction and attenuation responses in femtosecond region with an observed low transmittance value (~35%) at the high laser power above 80–650 GW/cm^2 (3). The phenomena were attributed to large fs 2PA cross-section values of C_{60}(>DPAF-C_9)$_2$ and C_{60}(>DPAF-C_9)$_4$ in the given concentration and, apparently, correlated to a higher number of DPAF-C_9 antenna in the structure of C_{60}(>DPAF-C_9)$_4$. The result also implied good photostability of these nanomaterials at high laser light energy. Evidently, there were new interesting findings of concentration-dependent effects on the nonlinear photonic characteristics of the materials, in terms of increasing two-photon absorption cross-section values at a low concentration. For example, as the concentration was decreased to 1.0×10^{-4} M from 1.0×10^{-2} M, a clear monotonous increase of the σ_2 value change ($\Delta\sigma_2$) was detected in a quantity from 13.9, 33.2, to 48.1 and 68.2×10^{-48} cm^4.sec.photon^{-1}.molecule^{-1}, or 1390, 3320, 4810, and 6820 GM, respectively, upon the structural variation from C_{60}(>DPAF-C_9), C_{60}(>DPAF-C_9)$_2$, to C_{60}(>DPAF-C_9)$_4$, respectively (3). We interpreted the concentration-dependent phenomena by the high tendency of C_{60}-*keto*-DPAF-C_9 chromophores to form nanoscaled aggregates in a concentration above 1.0×10^{-3} M. The driving force for this type of aggregation arises from strong fullerenyl π-interactions among C_{60} cage moieties forming an ordered molecular assembly. Even though the main aromatic ring structure of DPAF-C_9 antenna is planar, the molecular structural array of C_{60}(>DPAF-C_2) was found to follow the unit cell packing of fullerene cages, as shown in the single crystal structure of C_{60}(>DPAF-C_2) (1,5–6). Therefore, we expect the occurrence of cluster

Address correspondence to: Long Y. Chiang, Department of Chemistry, University of Massachusetts Lowell, Lowell, MA 01854. Tel: (978)-934-3663; Fax: (978)-934-3013; E-mail: Long_Chiang@uml.edu

formation of $C_{60}(>DPAF\text{-}C_9)_x$ in solution during the sample preparation when strong tendency of hydrophobic attraction among fullerene cages, via intermolecular *van der Waals* interactions, becomes effective. The phenomenon may exist even in a fairly dilute solution in a concentration below 1.0×10^{-4} M. The ability of C_{60}-*keto*-DPAF-C_9 chromophores to aggregate is highly influenced by their solubility in various solvents. Thus, high solubility of $C_{60}(>DPAF\text{-}C_9)_x$ in nonpolar solvents, such as toluene and CS_2, should lead to small coalescent particles as compared with those in polar solvents, such as benzonitrile and DMF. We also proposed that starburst structures as exemplified by $C_{60}(>DPAF\text{-}C_9)_4$ in a multipolar arrangement resembling encapsulation of C_{60} by four DPAF-C_9 antenna groups should provide a useful means to increase the degree of molecular dispersion and solubility. In general, quantum photoefficiency of $C_{60}(>DPAF\text{-}C_9)_x$ can be considerably depleted in the form of large solid particles and clusters over several microns in size that reduces their nonlinear optical efficiency significantly. In other words, controlled formation of well-organized and ordered nanoparticles (7) may, instead, enhance collective nonlinear photonic efficiency if a large surface area of nanoparticles becomes available for light-harvesting accumulation.

In this study, we evaluated the molecular assembly behavior in solution and the solvent-dependent and concentration-dependent aggregation particle size of the one-armed monoadduct $C_{60}(>DPAF\text{-}C_9)$, two-armed bisadduct $C_{60}(>DPAF\text{-}C_9)_2$, and four-armed tetraadduct $C_{60}(>DPAF\text{-}C_9)_4$ in toluene and CS_2 in correlation to their observed variation of nonlinear photonic properties upon the change of solution concentration.

2. Experimental

2.1. *Materials*

All C_{60}-*keto*-DPAF-C_9 conjugates used in this study, including the monoadduct C_{60}[methanocarbonyl-7-(9,9-di(3,5,5-trimethylhexyl)-2-diphenylaminofluorene)] $C_{60}(>DPAF\text{-}C_9)$, the bisadducts C_{60}[methanocarbonyl-7-(9,9-di(3,5,5-trimethylhexyl)-2-diphenylamino-fluorene)]$_2$ $C_{60}(>DPAF\text{-}C_9)_2$, and the tetraadducts C_{60}[methano carbonyl-7-(9,9-di(3,5,5-trimethylhexyl)-2-diphenylamino fluorene)]$_4$ $C_{60}(>DPAF\text{-}C_9)_4$ were prepared according to the literature procedure (1,8) (Figure 1).

2.2. *Dynamic Light Scattering (DLS) measurements of particle sizes*

Particle diameters were measured using a Malvern Zetasizer Nano ZS (Worcestershire, United Kingdom) instrument with the capability of detecting a particle size ranging from 0.6 nm to 6.0 μm. A 4.0 mW He-Ne laser light source (Class 1 compliant, EN 60825-1:2001 and CDRH) at 633 nm was applied and pumped through the sample solution, and subsequently detected by an Avalanche photodiode at 633 nm with Q.E > 50%. The laser attenuator was automatic with transmission from 100% to 0.0003%. The facility was purged with dry air as the condensation control. The temperature of the sample was kept at 25 °C.

The Malvern Nano Zetasizer instrument applies a noninvasive dynamic light scattering (DLS) technique for measuring the size of molecules and particles in solution, typically in the submicron region. The capability is extended for the measurement of a particle size lower than 1.0 nanometer due to the highest sensitivity available on the system. Its particle characterization involves a combination of zeta potential**,** particle size, and molecular weight with the particle size detecting range in between 0.6 nm and 6.0 μm**,** zeta potential range in between 3.0 nm and 10 μm, and the molecular weight range between 1.0×10^3 and 2.0×10^7 Da. Its use for the measurement in this study allowed us to detect the smallest assembly particle of $C_{60}(>DPAF\text{-}C_9)_x$ samples in solution.

2.3. *Transmission Electron Microscopic (TEM) measurements*

Procedure for the sample preparation is described as follows. A $C_{60}(>DPAF\text{-}C_9)_x$ sample with a calculated sample weight for the predefined concentration was placed in the test tube. To it was added either toluene or CS_2 (1.0 ml). The mixture was treated by sonication for a period of 1.5 h. A tin container with a 1000 carbon grid was used for the freeze-dry preparation of the sample. It was cooled with liquid nitrogen prior to the deposition of the sample solution (20 μl) onto the carbon grid. The container was then placed in a vacuum apparatus for solvent removal while under cooling.

3. Results and discussion

The chemical structure of $C_{60}(>DPAF\text{-}C_9)_x$ compounds consists of a C_{60} cage, a highly photoactive fluorene ring, and two sterically hindered 3,5,5-trimethylhexyl alkyl arms, where the fullerene cage and fluorene ring serve as an acceptor and a donor component, respectively. Electron-donating capability of the fluorene moiety was enhanced by the chemical attachment of an electron-releasing diphenylamino group at the C_2 position. That resulted in the induced molecular polarization upon photoexcitation with the π-electrons being polarized from the fluorene ring region to the C_{60} cage region. This photoinduced electronic polarization effect forms the fundamental basis of observed nonlinear photonic properties of $C_{60}(>DPAF\text{-}C_9)_x$ nanomaterials (9–10). However, the photoexcitation processes and optical effect rely greatly on the efficient light exposure of the molecule in the form of nanoparticles. Undesirable excessive molecular aggregation into large solid particles

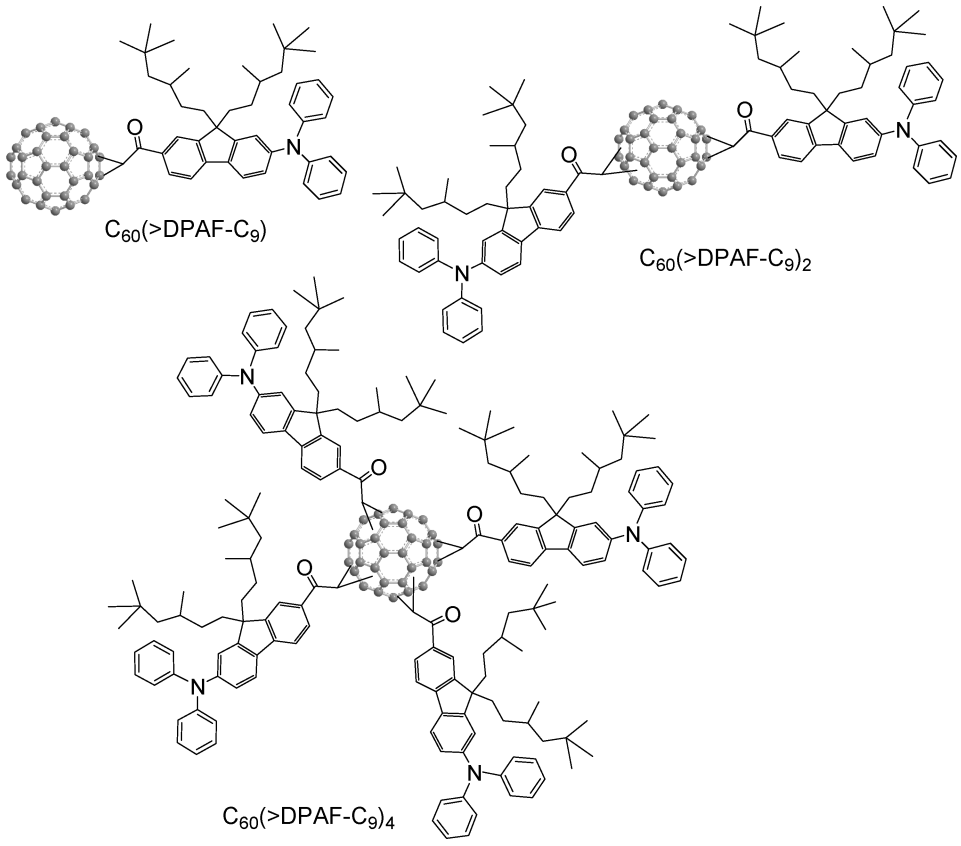

Fig. 1. The molecular structure of C_{60}(>DPAF-C_9), C_{60}(>DPAF-C_9)$_2$, and C_{60}(>DPAF-C_9)$_4$ compounds.

often restricts a significantly large quantity of molecules located at the inner particle region from the light exposure that makes them inactive during the photophysical excitation processes. Therefore, a suitable sample solution preparation method to minimize the formation of large solid particles over several microns becomes critical for acquiring the optimum photonic responses.

Synthesis of the monoadduct C_{60}(>DPAF-C_9) was carried out by a four-step reaction procedure starting from 2-bromofluorene via dialkylation at C_9 position of fluorene ring and followed by the attachment of a diphenylamino group at C_2 position of the resulting dialkylated fluorene moiety. The dialkyldiphenylaminofluorene (DPAF-C_n) intermediate formed was subsequently acylated by a α-bromoacetyl group at C_7 position of the fluorene ring to give the corresponding BrDPAF-C_n intermediate. Subsequent cyclopropanation of BrDPAF-C_n with C_{60} in the presence of a DBU base was followed to afford C_{60}(>DPAF-C_9) as brown solids. In the case of the bisadduct C_{60}(>DPAF-C_9)$_2$ or tetraadduct C_{60}(>DPAF-C_9)$_4$ preparation, a corresponding quantity of 2.2 or 4.4 equivalents, respectively, of the BrDPAF-C_n intermediate per C_{60} cage was applied (1). These products were purified via thin-layer chromatography.

A solution of C_{60}(>DPAF-C_9), C_{60}(>DPAF-C_9)$_2$, and C_{60}(>DPAF-C_9)$_4$ in either toluene or CS_2 was prepared at a concentration of 1.5×10^{-3}, 3.7×10^{-3}, and 1.0×10^{-2} M for the DLS measurements. Since a Zetasizer instrument is not able to detect particles at the concentration below 1.0×10^{-4} M, this concentration of the sample was absent from the measurement. The solution was treated by sonication for a period of 1.5 h to ensure good sample dissolution. However, a certain amount of undissolved sample solids did exist in each final solution that led to our persistent detection of large solid particles in a spherical diameter size over 10 μm. Therefore, the peaks in this high diameter region were omitted for clarification of the plot.

Particle size measurements in this study are based on dynamic light scattering (DLS) of particles in suspension undergoing Brownian motion, which is induced by the bombardment by solvent molecules, that themselves are moving due to their thermal energy. Upon the irradiation of a laser light, the intensity of the scattered light fluctuates, as a particle diffuses within a fluid, at a rate that is dependent upon the size of the particles as smaller particles moving more rapidly by the solvent molecules. Therefore, we are measuring the hydrodynamic diameter of C_{60}(>DPAF-C_9), C_{60}(>DPAF-C_9)$_2$, and C_{60}(>DPAF-C_9)$_4$ molecules or assemblies in toluene and CS_2. The diameter obtained by this technique is that of a sphere having the same translational diffusion coefficient as the particle being measured. The translational diffusion coefficient will depend not only

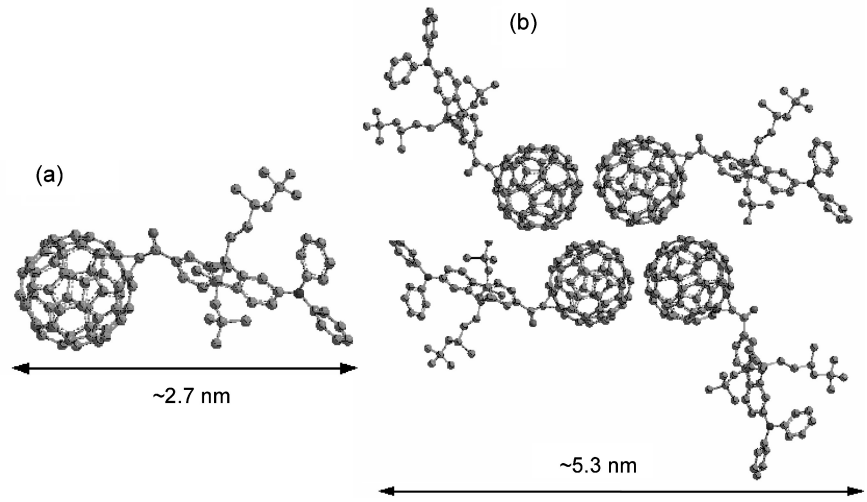

Fig. 2. The estimated long dimension length of (a) C_{60}(>DPAF-C_9) molecule and (b) the smallest molecular assembly of C_{60}(>DPAF-C_9) having 4–6 molecules in an array based on $C_{60}-C_{60}$ interactions, using 3D molecular modeling technique.

on the size of the particle "core" of C_{60}-DPAF moiety in the medium, but also on any 3,5,5-trimethylhexyl alkyl arm structures at the surface if the assembly is small. This means that the size obtained by this technique can be larger than that measured by transmission electron microscopy (TEM) method.

Dynamic light scattering measurements on all samples were performed by a number of repeated experiments. An average peak profile was calculated and plotted for the comparison among all figures shown. As a result, analysis and calculated particle sizes of C_{60}(>DPAF-C_9), C_{60}(>DPAF-C_9)$_2$, and C_{60}(>DPAF-C_9)$_4$, with the standard deviation value, at different concentrations in toluene were summarized in Table 1. The corresponding individual plots are displayed in Figures 3 and 4 with the averaged peak profile presented by a solid line.

The dimension length of each C_{60}(>DPAF-C_9) dyad molecule is estimated to be ~1.3 nm in the short dimension axis and ~2.7 nm in the long dimension axis, as shown in Figure 2a, using the 3D molecular modeling technique. Since the aromatic molecular core region of C_{60}(>DPAF-C_9) is rather rigid with conjugative bonds, the derived long dimension length based on the calculation of the bond lengths and the bond angles should be approximately accurate. As the C_{60}(>DPAF-C_9) molecules begin to assemble in solution owing to strong π-interaction of C_{60} cages, direct contact of six cages occupied at the six vertex sites of a octahedral shape is proposed to be the driving force for the formation of a smallest molecular assembly particle of C_{60}(>DPAF-C_9). The diameter dimension of this particle is estimated to be ~5.3 nm (Figure 2b).

Table 1. The particle sizes in diameter of C_{60}(>DPAF-C_9), C_{60}(>DPAF-C_9)$_2$, and C_{60}(>DPAF-C_9)$_4$ samples at different concentrations in toluene, measured by dynamic light scattering technique on a Zetasizer Nano instrument.

Sample	*Concentration*	*Small Particle (nm)*	*Large Particle (nm)*
C_{60}(>DPAF-C_9)	1.0×10^{-2} M	2.1 ± 0.3	>6.0 μm
	3.7×10^{-3} M	11 ± 0	70 ± 20
	1.5×10^{-3} M	4.0 ± 1.0	>1.0 μm
C_{60}(>DPAF-C_9)$_2$	3.7×10^{-3} M	17 ± 2.0	
	1.5×10^{-3} M	16 ± 2.0	290 ± 50
C_{60}(>DPAF-C_9)$_4$	1.0×10^{-2} M	9.0 ± 2.0	560 ± 50
	3.7×10^{-3} M	8.7 ± 0.2	300 ± 50
	1.5×10^{-3} M	7.5 ± 0.4	600 ± 300

Interestingly, regardless of the concentration of either 1.0×10^{-3} M (Figure 3Ac) or 1.0×10^{-2} M (Figure 3Aa), the assembly of C_{60}(>DPAF-C_9) molecules in toluene formed either a small nanoparticle size of ~4.0 ± 1.0 nm in diameter consistent with the size of the molecular packing described in Figure 2b or a large particle aggregate with a diameter size over 1.0 μm (Figure 3Ac). These large-sized particles increases to over 6.0 μm in diameter as the concentration reaches 1.0×10^{-2} M (Figure 3Aa). Apparently, no particles in an intermediate diameter size between 20 and 700 nm were detected, indicating a strong bimodal particle-size distribution in this solution system.

In the case of C_{60}(>DPAF-C_9) molecules in CS_2 at the concentration of 1.5×10^{-3} M (Figure 4Bb), the majority of nanoparticles was formed in a diameter size of ~7.0 nm and ~75 nm also in a bimodal particle-size distribution. Particles in a larger size of two were found to increase to ~300 nm and >4.0 μm in diameter in a trimodal particle-size distribution upon the increase of the concentration to 1.0×10^{-2} M. As the structure of C_{60}-*keto*-DPAF-C_9 changes to the bisadduct C_{60}(>DPAF-C_9)$_2$, two molecular assemblies with a bimodal particle-size distribution of either 16 ± 2.0 nm or 290 ± 50 nm in diameter were

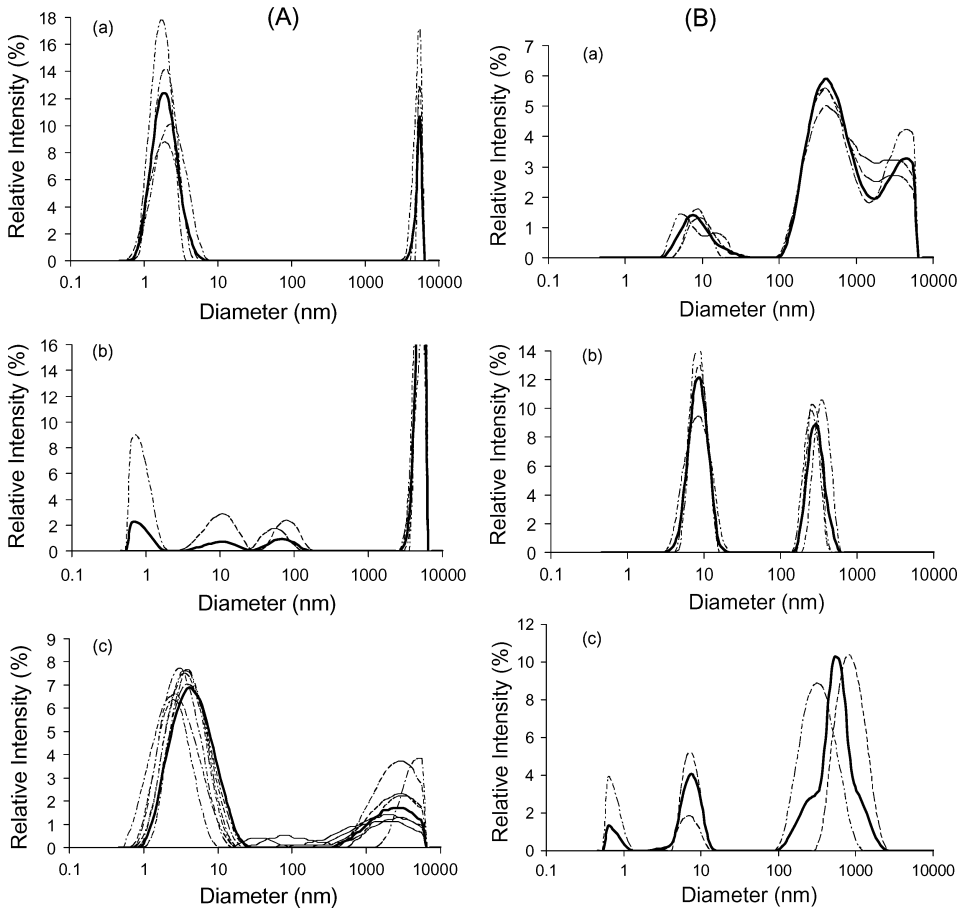

Fig. 3. Dynamic light scattering measurements for the particle size in diameter of (A) C_{60}(>DPAF-C_9) and (B) C_{60}(>DPAF-C_9)$_4$ at the concentration of (a) 1.0×10^{-2} M, (b) 3.7×10^{-3} M, and (c) 1.5×10^{-3} M, showing a bimodal peak profile in the most cases in the region between 2.0 nm and 6.0 μm.

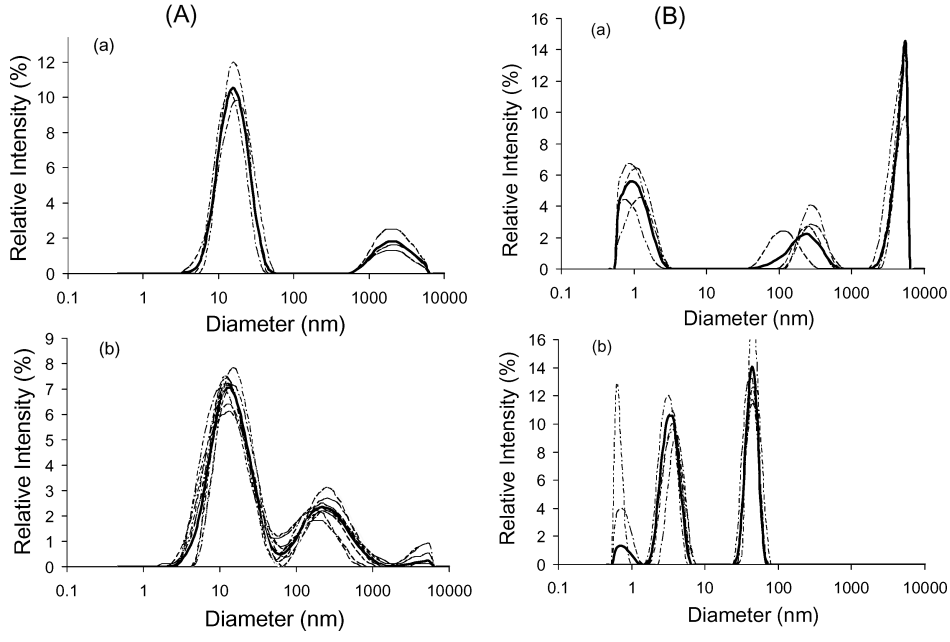

Fig. 4. Dynamic light scattering measurements of (A) C_{60}(>DPAF-C_9)$_2$ at the concentration of (a) 3.7×10^{-3} M and (b) 1.5×10^{-3} M in toluene and (B) C_{60}(>DPAF-C_9) at the concentration of (a) 1.0×10^{-2} M and (b) 1.5×10^{-3} M in CS_2, showing the peak of particle-size in diameter.

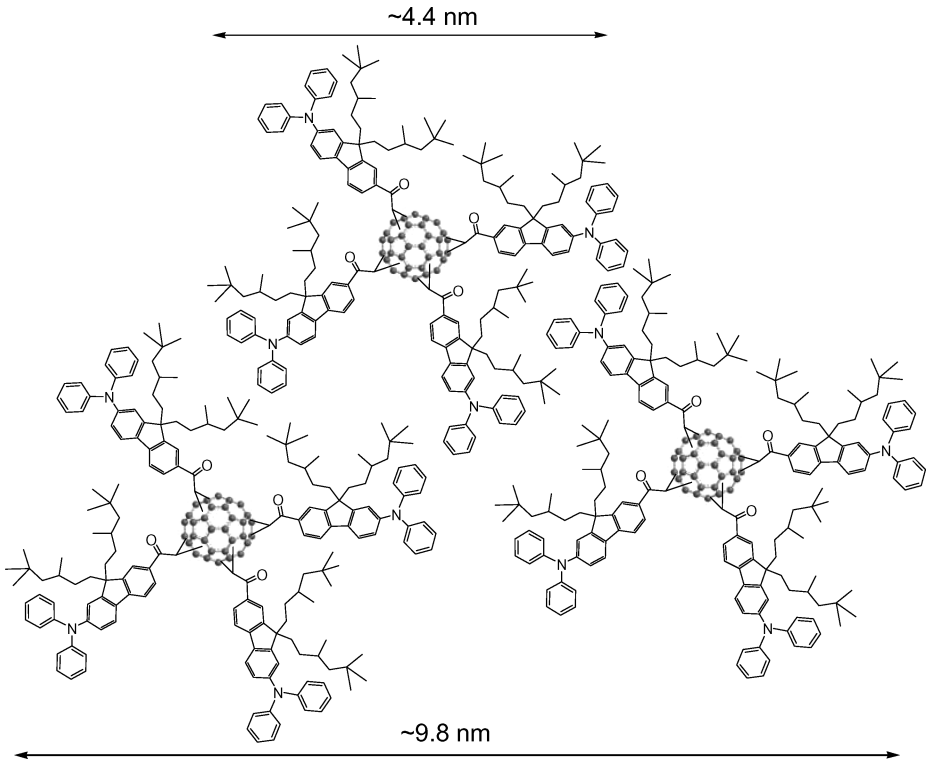

Fig. 5. The estimated long dimension length of the $C_{60}(>DPAF\text{-}C_9)_4$ molecular assembly having 3–6 molecules packed in a nanoparticle.

found at the concentration of 1.5×10^{-3} M in toluene (Figure 4Ab). The larger one of these two particle-size distributions moved up to ~2.5 μm in diameter as the concentration increased to 3.7×10^{-3} M (Figure 4Aa).

The molecular assembly of the tetraadduct $C_{60}(>DPAF\text{-}C_9)_4$ in toluene at the concentration of either 3.7×10^{-3} or 1.5×10^{-3} M formed two sizes of particles in a bimodal distribution with the diameter lengths centered at 8.7 ± 0.2 or 7.5 ± 0.4 nm, respectively, and 300 ± 50 or 600 ± 300 nm, respectively, as shown in Figures 3Bb and 3Bc. Intensity of the smaller particle size of these two peaks was found to decrease while the larger particle-size peak shifted partially to even larger sizes over 4.0 μm in diameter (Figure 3Ba). Notable change in intensity among these peaks indicated the systematic tendency of larger particle formation at a concentration of 1.0×10^{-2} M. Interestingly, the former small diameter size agrees well with the estimated long dimension length of the $C_{60}(>DPAF\text{-}C_9)_4$ molecular assembly as ~9.8 nm, having 3–6 molecules packed in a nanoparticle (Figure 5), indicating clearly the fundamental nature of $C_{60}(>DPAF\text{-}C_9)_4$ self-assembly by a loose packing of DPAF-C_9-antenna-encapsulated C_{60} nanostructures.

4. Conclusions

We have studied the molecular self-assembly tendency of $C_{60}(>DPAF\text{-}C_9)$ dyad, $C_{60}(>DPAF\text{-}C_9)_2$ triad, and $C_{60}(>DPAF\text{-}C_9)_4$ pentads in solvent-dependent and concentration-dependent manner. The evaluation was performed by the particle-size measurements on molecular assemblies in either toluene or CS_2 using the dynamic light scattering technique. As a result, we observed a strong bimodal particle size distribution in the most cases of the samples in both nonpolar solvents. In the instance of $C_{60}(>DPAF\text{-}C_9)$ dyad, the first group of small nanoparticles exhibited a particle diameter size of 3.0–4.0 nm in good agreement with the estimated long axis length of $C_{60}(>DPAF\text{-}C_9)$ (~2.7 nm), using 3D molecular modeling technique. Similar observation of a bimodal particle size distribution was detected on $C_{60}(>DPAF\text{-}C_9)_4$ pentads in toluene with a small nanoparticle diameter size of ~8.0 nm fitting well with the estimated dimension length of ~9.8 nm for loosely packed 3–6 $C_{60}(>DPAF\text{-}C_9)_4$ molecular assemblies. Furthermore, the tendency of forming large aggregation particles in a particle diameter of more than 4.0 μm was significantly enhanced at a high concentration of 1.0×10^{-2} M.

Acknowledgements

We thank the Air Force Office of Scientific Research for funding under the contract number FA9550-05-1-0154.

References

1. Padmawar, P.A., Canteenwala, T., Tan L.-S., Chiang, L.Y. (2006) *J. Mater. Chem*., 16: 1366–1378.
2. Padmawar, P.A., Rogers, J.O., He, G.S., Chiang, L.Y., Canteenwala, T., Tan, L.-S., Zheng, Q., Lu, C., Slagle, J.E., Danilov, E., McLean, D.G., Fleitz P.A., Prasad, P.N. (2006) *Chem. Mater*., 18: 4065–4074.
3. Elim, H.I., Anandakathir, R., Jakubiak, R., Chiang, L.Y., Ji, W., Tan, L.S. (2007) *J. Mater. Chem.*, 17: 1826–1838.
4. El-Khouly, M E.; Anandakathir, R., Ito, O., Chiang, L.Y. (2007) *J. Phys. Chem. A*, 111: 6938–6944.
5. Chiang, L.Y., Padmawar, P.A., Canteenwala, T., Tan, L.-S., He, G.S., Kannan, R., Vaia, R., Lin, T.-C., Zheng, Q., Prasad, P.N. (2002) *Chem. Comm*., 1854–1855.
6. Padmawar, P.A., Canteenwala, T., Sarika, V., Tan L.-S., Chiang, L. Y. (2004) *J. Macromol. Sci. A, Pure and Appl. Chem*., 41: 1387–1400.
7. Verma, S., Hauck, T., El-Khouly, M.E., Padmawar, P.A., Canteenwala, T., Pritzker, K., Ito, O., Chiang, L.Y. (2005) *Langmuir*, 21: 3267–3272.
8. Padmawar, P.A., Canteenwala, T., Verma, S., Tan, L.-S., He, G.S., Prasad, P.N., Chiang, L.Y. (2005) *Synth. Met*., 154: 185–188.
9. Luo, H., Fujitsuka, M., Araki, Y., Ito, O., Padmawar, P., Chiang, L.Y. (2003) *J. Phys. Chem. B*, 107: 9312–9318.
10. El-Khouly, M.E., Padmawar, P., Araki, Y.; Verma, S., Chiang, L.Y., Ito. O. (2006) *J. Phys. Chem. A*, 110: 884–891.